Hindawi Publishing Corporation
Journal of Sensors
Volume 2010, Article ID 487061, 5 pages
doi:10.1155/2010/487061

*Research Article*

# $Ta_2O_5$ Thin Films for Capacitive RF MEMS Switches

**Anna Persano,[1] Fabio Quaranta,[1] Adriano Cola,[1] Antonietta Taurino,[1] Giorgio De Angelis,[2] Romolo Marcelli,[2] and Pietro Siciliano[1]**

[1] *CNR-IMM, Institute for Microelectronics and Microsystems-Unit of Lecce, National Council of Research, Via Monteroni, 73100 Lecce, Italy*

[2] *CNR-IMM, Institute for Microelectronics and Microsystems-Unit of Roma, National Council of Research, Via del Fosso del Cavaliere 100, 00133 Roma, Italy*

Correspondence should be addressed to Anna Persano, anna.persano@le.imm.cnr.it

Received 31 August 2010; Accepted 7 December 2010

Academic Editor: Yongxiang Li



Shunt capacitive RF MEMS switches have been developed using III-V technology and employing (tantalum pentoxide) $Ta_2O_5$ thin films as dielectric layers. In order to evaluate the potential of the $Ta_2O_5$ thin films for the considered application, the compositional, structural, and electrical characterization of the deposited films has been performed, demonstrating that they are good candidates to be used as dielectric layers for the fabrication of RF MEMS switches. Specifically, $Ta_2O_5$ films are found to show a leakage current density of few nA/cm$^2$ for $E \sim 1$ MV/cm and a high dielectric constant of 32. Moreover, the charging process has been investigated, finding that it follows a stretched exponential law. The fabricated switches show actuation voltages in the range 15–20 V, an insertion loss better than $-0.8$ dB up to 30 GHz, and an isolation of $\sim -40$ dB at the resonant frequency which is around 25 GHz.

## 1. Introduction

Radio frequency (RF) microelectromechanical system (MEMS) switches are very attractive for their potential of overcoming the limits of the traditional solid-state devices (pin-diode, FET-switches) thanks to the very low insertion loss and power dissipation, high isolation and linearity which are provided by the electrostatic actuation of the suspended membrane [1]. On the other hand, PIN diodes and FETs have a characteristic capacitance that is due to their physical dimensions, which can reduce the amount of isolation available in their off states at high frequencies. To compensate for the poor isolation devices can be manufactured with reduced capacitance with the drawback that the "on" resistance of the devices increases, resulting in high insertion losses of PIN and FET-based systems. Moreover, another important advantage of the RF MEMS switches is their ability to be manufactured with MMIC processes on any substrate material including silicon, gallium arsenide, and alumina.

In spite of the attractive capabilities, the reliability of RF MEMS switches is still an open issue because of the limitations mainly due to the charging mechanisms in the dielectric material used to cover the actuation pads which affect the collapse of bridges and cantilevers [2–5]. Specifically, in capacitive MEMS switches when the pull-down voltage is applied and the bridge comes in contact with the dielectric, which is usually $Si_3N_4$ in III-V technology, charge carriers are injected and then trapped in the dielectric layer. Even though the exact mechanisms for the transfer and trapping of charge are not known, the effects are measurable resulting in a change in the pull-down voltage and/or in the phenomenon of stiction which seriously limits the functionality of devices. This is because when charge becomes trapped within the dielectric, it tends to screen the applied electric field that is used to control the actuation and release of the switch. More specifically, as the charge builds up, the screening voltage detracts from the actuation voltage until there is no longer enough force pulling down the membrane to cause it to actuate. The opposite occurs when the actuation voltage is removed and the trapped charge provides enough potential to stick down the membrane. The dielectric constant of the isolation layer covering the actuation line in the capacitive switches determines the ratio between the capacitance of the switch in the down and up state ($C_{down}/C_{up}$). This capacitance ratio is an important figure of merit for RF MEMS switches [6].

In order to overcome the limitations of RF MEMS switch reliability due to the electric/dielectric properties of the isolation layers and, hence, to optimize the switch performance, the investigation of dielectric materials which can be alternative to the ones commonly used becomes mandatory.

In this paper tantalum pentoxide ($Ta_2O_5$) thin films have been investigated for application as dielectric layers in RF MEMS switches realized in III-V technology. In order to optimize the deposition of the $Ta_2O_5$ thin films for the considered application, a comprehensive characterization of the compositional, morphological, structural, and electric/dielectric properties of the films has been performed. In particular, dielectric charging process, whose understanding is essential to evaluate the application of a dielectric material in RF MEMS switches, has been investigated by performing capacitance and current transients. The charging effects have been investigated in $Si_3N_4$ [4] while, to the best of our knowledge, they have not yet been addressed in $Ta_2O_5$ thin films. A fabrication process compatible with the III-V technology has been developed for the realization of shunt capacitive RF MEMS switches with $Ta_2O_5$ films as dielectric layers. Finally, the fabricated switches have been characterized in the RF domain.

## 2. Material Characterization

$Ta_2O_5$ thin films were deposited by RF-magnetron reactive sputtering from a high-purity tantalum metal target (4 inch diameter). The $Ta_2O_5$ films were prepared at a fixed power of 200 W and with a chamber pressure of 9 mTorr. A flow ratio of 1 : 2 in the sputtering gas mixture of argon and oxygen was used.

In order to perform the $Ta_2O_5$ film electrical characterization, test capacitors with a metal-insulator-metal (MIM) structure were fabricated on (100) semi-insulating GaAs substrates Figure 1(a). Both bottom and top MIM metallizations were deposited by magnetron reactive sputtering in a separate vacuum system. The bottom contact is a continuous multilayer Ti/Au/Ti (10/100/10 nm) over the wafer. The top electrode consists of square Ti/Au (10/300 nm) contacts with a 180-$\mu$m size which were realized by standard optical lithography. The $Ta_2O_5$ film thickness was measured by using an Alpha–Step IQ and results to be $324 \pm 5$ nm.

The structure and the composition of the deposited $Ta_2O_5$ films were analyzed by using X-ray diffraction and X-ray photoelectron spectroscopy, respectively. The films were found to be amorphous with a composition almost stoichiometric (ratio O/Ta = 2.46).

$Ta_2O_5$ film morphology was investigated by plan-view and cross-sectional scanning electron microscopy (SEM) analyses. A Zeiss NVISION 40 dual beam Focused Ion Beam (FIB), equipped with a high-resolution SEM GEMINI column, was used to analyze the surface morphology of the $Ta_2O_5$film, where not covered by the Au metal layer, as well as to prepare FIB cross-section for the inspection of the layer stack in the region of the MIM capacitors. The surface of the $Ta_2O_5$film turned out to be quite flat and homogeneous, as shown in Figure 1(b), whereas the cross-sectional analyses revealed a $Ta_2O_5$ film compact and continuous over the whole capacitor region [Figure 1(c)].

Charging effects in the $Ta_2O_5$ films were investigated by performing capacitance and current transients under a constant applied electric field.

All electric measurements were performed at room temperature in an electromagnetically shielded K. Suss PM5 Probe Station. The capacitance transients were measured by using a HP4284A precision LCR-meter with a sinusoidal excitation voltage having an amplitude of 30 mV at the frequency of 1 MHz. The current transients were measured by using two low-noise preamplifiers connected to a 4200 Keithley parametric system in order to apply a positive bias voltage at the upper contact of MIM structures and measure the current at the bottom electrode. The current detection limit in our measurements was ~2 fA.

Figure 2 shows that the capacitance decays over time, as already reported in charging studies on $Si_3N_4$ films in capacitive RF MEMS switches [3]. These capacitance transients are attributed to the fact that the charge injected under the application of the electric field can be trapped in the large density of defect states contained in the dielectric film, causing a change in the dielectric polarization which follows a stretched exponential law [3]

$$P(t) = P_i \exp\left[-\left(\frac{t}{\tau}\right)^{\beta}\right], \quad (1)$$

where $P_i$ is the initial polarization, $\tau$ is the process time constant, and $\beta (0 \leq \beta \leq 1)$ is the stretch factor. According the given interpretation, the capacitance results in a temporal decay expressed by:

$$C(t) = C_{\infty} + \Delta C \exp\left[-\left(\frac{t}{\tau}\right)^{\beta}\right], \quad (2)$$

where $C_{\infty}$ is the steady-state capacitance after the application of the voltage and $\Delta C$ is the transient amplitude. In Figure 2, the fit line of (2) to the experimental $C(t)$ transient at $E = 0.9$ MV/cm is shown. The fitting parameters $\tau$ and $\beta$ are found to be $1.24 \times 10^8$ s and 0.18, respectively. When the applied field is zero ($E = 0$) the capacitance value is 28.77 pF.

Steady-state capacitance was found to be mainly independent of the voltage and, according to the usual approximation, it is given by the geometric expression $C = \varepsilon_s \varepsilon_0 A/d$, where $\varepsilon_s$ is the static dielectric constant of the insulator, $\varepsilon_0$ is the permittivity of free space, $A$ is the active area ($180 \times 180\,\mu m^2$) and $d$ is the film thickness. We estimate a static dielectric constant value $\varepsilon_s = 32$, in agreement with the values reported for $Ta_2O_5$ films [7]. This dielectric constant value is much higher than that of $Si_3N_4$ (6-7) which is the dielectric material commonly used in capacitive RF MEMS switches. The high dielectric constant is appealing for the application of $Ta_2O_5$ as dielectric material in capacitive switches since it allows to significantly increase the capacitance ratio $C_{down}/C_{up}$ [6].

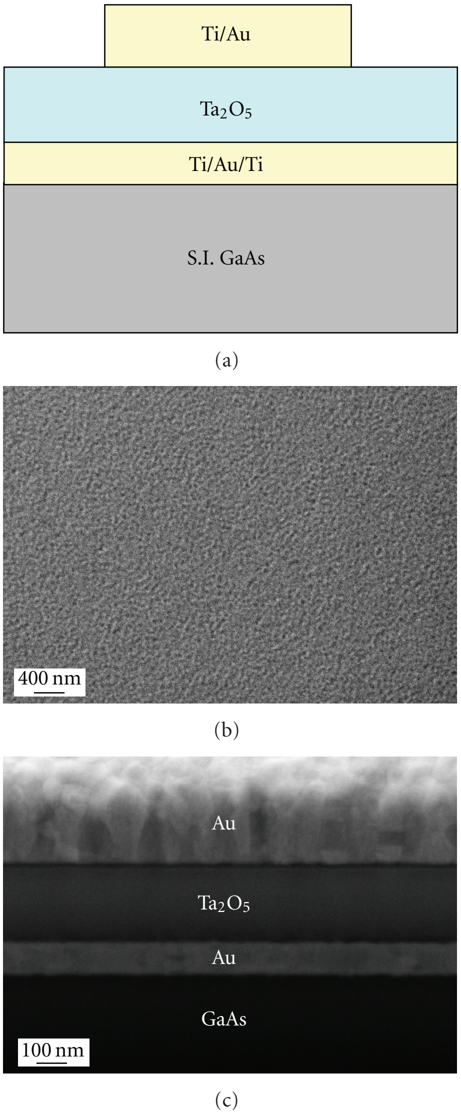


FIGURE 1: (a) Sketch of the $Ta_2O_5$-based MIM capacitors. (b) Plan view SEM image of the $Ta_2O_5$ surface. (c) Cross-sectional image of a $Ta_2O_5$-based MIM structure.

Charge trapping is also responsible for a reduction of the leakage current due to a screening of the applied electric field. Specifically, the temporal variation of the polarization expressed by (1) has been reported in the literature to give rise to current transients expressed by [4]

$$J(t) \propto \frac{\beta}{\tau}\left(\frac{t}{\tau}\right)^{\beta-1} \exp\left[-\left(\frac{t}{\tau}\right)^{\beta}\right] \tag{3}$$

Current transients were recorded under the application of a constant step-like electric field, and they are obtained to be well fitted by (3). According to the previous interpretation, these current transients are due to the trapping of the injected carriers in the dielectric film. Figure 3 shows the current transient measured by applying 0.9 MV/cm and the fitting curve obtained by (3) with $\tau$ and $\beta$ equal to $2.9 \times 10^8$ s and 0.18, respectively. The steady-state leakage current density was found to be $\sim 0.1/(180\times180)$ pA/$\mu$m$^2$, being this value comparable with $Si_3N_4$ films [4]. The fitting parameter values found from current transients are close to those obtained from the fitting of capacitance transients, thus demonstrating that both capacitance and current transients are able to detect the same dielectric charging process. Further details of the analysis performed on the current transients are reported in [8].

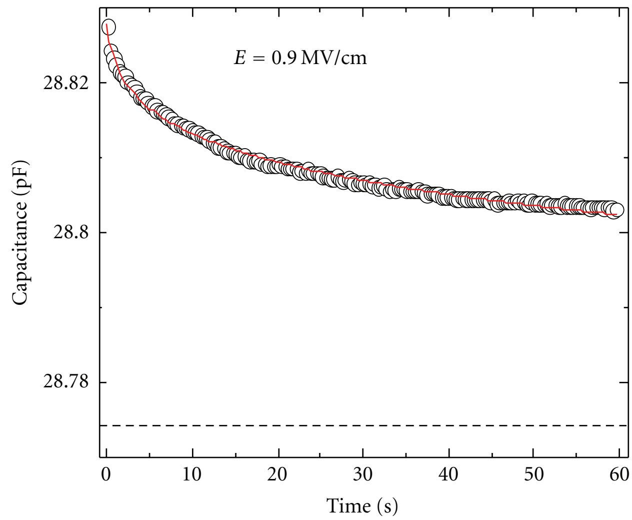


FIGURE 2: Typical capacitance transient during the application of a constant electric field $E = 0.9$ MV/cm. The solid line is the fit to the capacitance data with the (2).

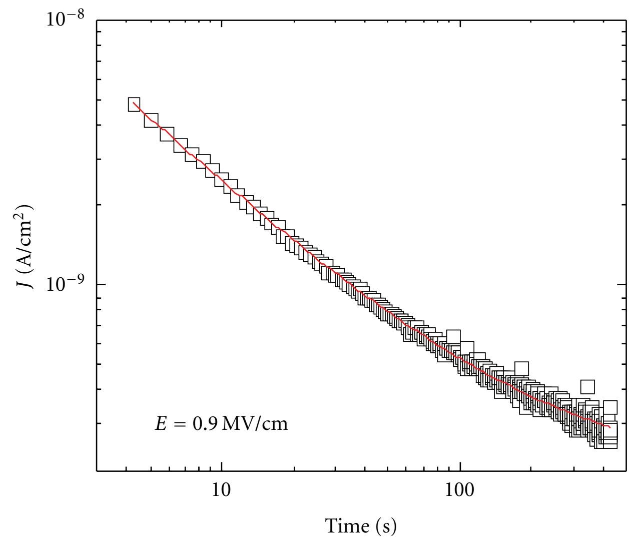


FIGURE 3: Typical current transient recorded by applying $E = 0.9$ MV/cm. The solid line is the fit to the current data with (3).

## 3. Switch Fabrication and RF Characterization

Shunt capacitive switches were fabricated in III-V technology using as dielectric layers the $Ta_2O_5$ thin films studied in Section 2.

For actuation lines another tantalum-based material which is the tantalum nitride (TaN) was used. A preliminary characterization of the compositional and electrical properties as a function of the deposition temperature and the sputtering gas mixture composition was also performed for TaN films, as reported in [9].

A surface-micromachined approach was followed for the fabrication of switches. They are in coplanar waveguide (CPW) configuration with a suspended metal bridge connecting the lateral ground planes and a dielectric layer on the central conductor which provides a capacitive contribution when the bridge is in down state.

The fabrication process can be described as follows. A 500-nm-thick $Si_3N_4$ layer was deposited as isolation layer over a semi-insulating GaAs substrate. Next, a 120-nm-thick TaN layer was deposited by sputtering at 25°C with a 20% content of $N_2$ in the gas feed mixture, and then it was patterned by a reactive ion etching (RIE) process based on fluorine chemistry (etching rate value of 28 nm/min) in order to define the actuation electrodes. A 400-nm-thick $Ta_2O_5$ was deposited and via holes were defined to contact the electrodes by standard optical photolithography and dry etching (fluorine-based chemistry). The dry-etching process is not selective with respect to the TaN; hence a previous optimization was performed. A metal multilayer of Ti/Pt/Au (30/30/60 nm) was then deposited on the $Ta_2O_5$ layer to realize underpass lines and the pads to contact the TaN electrodes by using lift-off technique. The metal was subsequently covered with another 400-nm-thick $Ta_2O_5$ dielectric layer. The sacrificial layer for the definition of the air gap under the bridges was formed by a 3-$\mu$m-thick photoresist. Another metal multilayer of Ti/Au/Ti (5/50/5 nm) was evaporated on the entire surface, to be used as electrical contact film and seed layer for the following electroplating deposition of 1-$\mu$m-thick gold layer using a gold cyanide bath. The bridges were grown with a set of aligned holes which allow the removal of the sacrificial layer using dry-etching techniques and a faster operation of the switch by reducing the air damping underneath the bridge. The holes have a squared shape with an area of typically $10 \times 10\,\mu m^2$ and a distance from each other of $\sim 10\,\mu$m. A second gold electroplating deposition with a 1.5-$\mu$m thickness was used to thicken the CPW lines, the ground pads, and to build up a frame to improve the flatness of the bridge. A combination of selective wet and dry etching was used to remove the unwanted Ti/Au/Ti multilayer among the devices. Finally, the air bridges were released by removing the underlying sacrificial photoresist by a high-pressure $O_2$ plasma process performed in a barrel etcher in order to prevent sticking problems. The process was divided in many steps in order to avoid the over-heating of membranes which can induce distortion effects.

Profilometer analysis showed that the bridges are enough robust for reliability purposes and flexible to be driven by reasonable (lower than $\sim$50 V) values of the applied voltage.

SEM images were also recorded in order to check the quality of the different process steps. An SEM plan-view of a fabricated switch is shown in Figure 4.

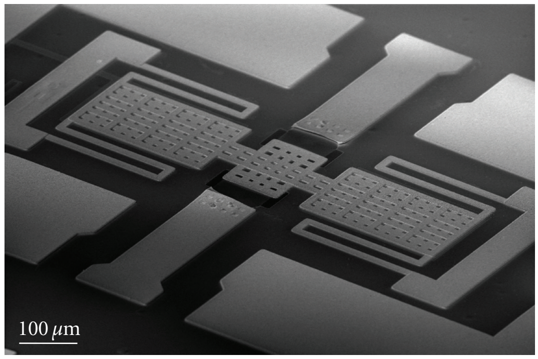


Figure 4: Plan-view SEM of a shunt capacitive RF MEMS switch fabricated on GaAs substrate using $Ta_2O_5$ thin films as dielectric layers.

A remotely controlled HP8510C vector network analyzer (VNA) together with a Karl Süss Probe Station equipped with ground-signal-ground RF $|Z|$-probes and DC probes was used for the measurement of the $S$-parameters of switches in the up and down states. Measurements were taken using a commercial short-open-load thru (SOLT) calibration with 801 points in a frequency range from 1 GHz to 40 GHz. Switch actuation voltages of 15–20 V were obtained by performing a voltage ramp with a rate of 1 V/sec. These actuation voltages are lower than the values (ranging from 30 to 80 V) reported today for most of the RF MEMS switches with the benefit that an increase of the switch lifetime can be achieved [2]. Finally, $S$-parameters in the down and up states were recorded.

Typical $S$-parameters in the up and down states are displayed in Figures 5 and 6, respectively. In the up state, the return loss is lower than −10 dB below 28 GHz, while the insertion loss is −0.2 dB at 20 GHz and better than −0.8 dB up to 30 GHz. In the down state, the return loss is better than −0.3 dB in almost all the measured frequency range and a resonant frequency of 23 GHz (isolation of −38 dB) is observed. The obtained results compare favourably with the $S$-parameters recently measured for shunt capacitive switches fabricated in III-V technology [10]. The value of the resonant frequency was found to reduce from $\sim$30 GHz to 15 GHz with increasing the bridge length in the range 450–750 $\mu$m, in agreement with the increasing of the inductive contribution [1].

## 4. Conclusion

$Ta_2O_5$ thin films have been used as dielectric layers in capacitive RF MEMS switches developed in III-V technology. A preliminary characterization of $Ta_2O_5$-based capacitors has been performed, allowing to address all the film properties (morphology, leakage current, dielectric constant, and charging mechanisms) which seriously affect the switch operation. Specifically, it has been found that $Ta_2O_5$ films are flat, compact, and continuous over the whole capacitor region. They show an interesting low leakage current density of few nA/cm$^2$ for $E \sim 1$MV/cm and a high dielectric constant

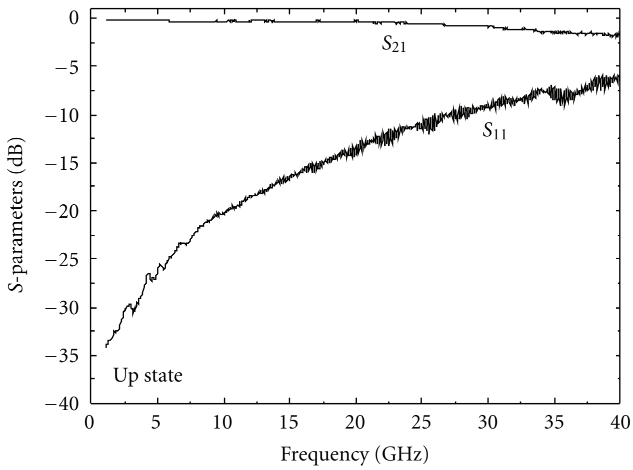


FIGURE 5: Insertion ($S_{21}$) and return ($S_{11}$) losses for a shunt capacitive switch in the up state.

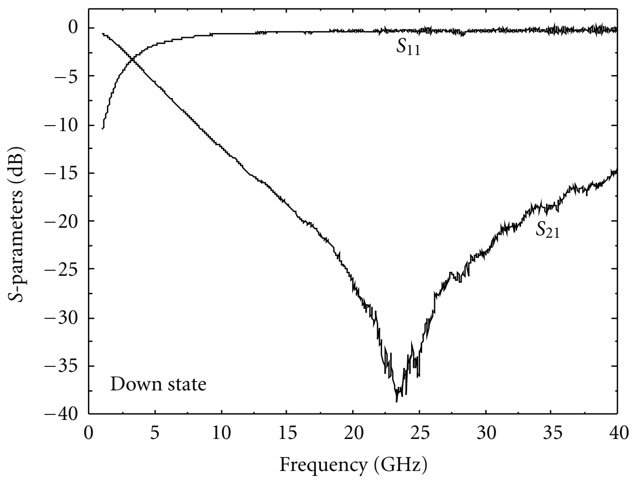


FIGURE 6: $S_{21}$ and $S_{11}$ parameters for a shunt capacitive switch in the down state.

of 32. All these results prove that the $Ta_2O_5$ can be a valid alternative to $Si_3N_4$ which is the standard dielectric material used in capacitive RF MEMS switches. Moreover, current and capacitance transients performed on the $Ta_2O_5$-based MIM capacitors show that the dielectric charging process follows a stretched exponential law. The understanding and the modelling of the dielectric charging is essential for its prediction and possible reduction when the dielectric material is employed in RF MEMS switches.

A fabrication process compatible with the III-V technology has been developed for the realization of capacitive RF MEMS switches with the $Ta_2O_5$ films. Finally, RF performance of the realized switches has been measured, finding S-parameters values which compare favorably with the results recently reported in the literature for capacitive switches in III-V technology.

The results presented here prove the potential of $Ta_2O_5$ thin films to be used in RF MEMS switches and provide useful information on device development.

## Acknowledgments

This work was supported in part by the Italian University and Reserch Ministry (MIUR) under FIRB Project no. DM25810. The authors thank Fondazione Bruno Kessler FBK, MEMS Research Unit, Povo TN, Italy, for providing the design of the switches realized in this work. M. C. Martucci and P. Cretí are also acknowledged for the technical support in the switch fabrication process.

## References

[1] G. Rebeiz, *RF MEMS Theory, Design, and Technology*, Wiley-Interscience, New York, NY, USA, 2003.

[2] C. Goldsmith, J. Ehmke, A. Malczewski et al., "Life time characterization of capacitive RF MEMS switches," in *Proceedings of the IEEE MTT-S International Microwave Symposium Digest*, pp. 227–230, Phoenix, Ariz, USA, May 2001.

[3] G. Papaioannou, M. N. Exarchos, V. Theonas, G. Wang, and J. Papapolymerou, "Temperature study of the dielectric polarization effects of capacitive RF MEMS switches," *IEEE Transactions on Microwave Theory and Techniques*, vol. 53, no. 11, pp. 3467–3473, 2005.

[4] U. Zaghloul, G. Papaioannou, F. Coccetti, P. Pons, and R. Plana, "Dielectric charging in silicon nitride films for MEMS capacitive switches: effect of film thickness and deposition conditions," *Microelectronics Reliability*, vol. 49, no. 9-11, pp. 1309–1314, 2009.

[5] N. Tavassolian, M. Koutsoureli, E. Papandreou et al., "The effect of silicon nitride stoichiometry on charging mechanisms in RF-MEMS capacitive switches," *IEEE Transactions on Microwave Theory and Techniques*, vol. 57, no. 12, Article ID 5332264, pp. 3518–3524, 2009.

[6] T. Lisec, C. Huth, and B. Wagner, "Dielectric material impact on capacitive RF MEMS reliability," in *Proceedings of the 12th Global Automotive Aftermarket Symposium (GAAS '04)*, pp. 471–474, Amsterdam, The Netherlands, 2004.

[7] S. Ezhilvalavan and T. Y. Tseng, "Conduction mechanisms in amorphous and crystalline $Ta_2O_5$ thin films," *Journal of Applied Physics*, vol. 83, no. 9, pp. 4797–4801, 1998.

[8] A. Persano, F. Quaranta, M. C. Martucci, P. Cretì, P. Siciliano, and A. Cola, "Transport and charging mechanisms in $Ta_2O_5$ thin films for capacitive RF MEMS switches application," *Journal of Applied Physics*, vol. 107, no. 11, Article ID 114502, 2010.

[9] A. Persano, F. Quaranta, A. Cola et al., "Alternative materials for RF MEMS switches in III-V technology," in *Proceedings of the Symposium on Design, Test, Integration and Packaging of MEMS/MOEMS (DTIP '10)*, pp. 295–298, Seville, Spain, May 2010.

[10] F. Crispoldi, A. Pantellini, S. Lavanga et al., "Full integrated process to manufacture RF-MEMS and MMICs on GaN/Si substrate," *International Journal of Microwave and Wireless Technologies*, vol. 2, no. 3-4, pp. 333–339, 2010.